

Article

# The Adsorption Kinetic Parameters of $\text{Co}^{2+}$ Ions by $\alpha\text{-C}_2\text{SH}$

Domante Niuniavaite, Kestutis Baltakys \* and Tadas Dambrauskas

Department of Silicate Technology, Kaunas University of Technology, Radvilenu road 19, LT-50270 Kaunas, Lithuania; domante.niuniavaite@ktu.edu (D.N.); tadas.dambrauskas@ktu.lt (T.D.)

\* Correspondence: kestutis.baltakys@ktu.lt; Tel.: +370-73-300163

Received: 24 November 2017; Accepted: 12 January 2018; Published: 15 January 2018

**Abstract:** In this work, the kinetic parameters of  $\text{Co}^{2+}$  ion adsorption by  $\alpha\text{-C}_2\text{SH}$  were determined.  $\alpha\text{-C}_2\text{SH}$  was synthesized under hydrothermal conditions at  $175\text{ }^\circ\text{C}$ , when the duration of isothermal curing was 24 h and the molar ratio of primary mixture was  $\text{CaO}/\text{SiO}_2 = 1.5$ . This research allows us to state that the adsorption reactions proceed according to the chemisorption process. In order to determine adsorption kinetic parameters, kinetics models have been developed and fitted for these reactions. Additionally, it was determined that adsorbed  $\text{Co}^{2+}$  ions have a significant influence on the stability of  $\alpha\text{-C}_2\text{SH}$ . These results were confirmed by XRD, STA, and atomic absorption spectroscopy methods.

**Keywords:** calcium silicate hydrate; heavy metals ions; adsorption; kinetics

## 1. Introduction

Heavy metal pollution in wastewater is one of the most serious environmental problems because most of it is toxic, even at very low concentrations [1–4]. This pollution appears in many industries, such as metal plating, mining operations, chlor-alkali, radiator manufacturing, and alloy industries [2,5,6]. Methods for removing metal ions from aqueous solutions mainly consist of physical, chemical, and biological technologies [1,7]. Various treatment processes have been developed for the removal of metal ions: chemical precipitation, filtration, ion exchange, electrochemical treatment, membrane technologies, and evaporation [8–10]. Among these methods, adsorption is attractive due to its low cost, high efficiency, and simple operation [11,12]. The common adsorbents primarily include activated carbon, zeolites, bio macromolecules, and calcium silicate hydrates [12–15]. However, some adsorbents show low adsorption capacities and short operation time [3,12]. In addition, when these adsorbents reach their adsorption capacity limit, they are usually stored to a landfill and discarded, which eventually causes secondary pollution due to the risk of leaching and the subsequent release of non-biodegradable heavy metals [16]. For these reasons, the research on new adsorbents that can be used as additives in ordinary Portland cement or in the manufacture of alternative cementitious materials is in progress [17].

Calcium silicate hydrates (CSH) play important roles in many areas: in drug delivery, bone tissue engineering, the cement industry, and adsorption for heavy metal ions [12,18,19]. It is known that low basicity calcium silicate hydrates (gyrolite and tobermorite) have good adsorption properties for some metal ions [20,21]. To our knowledge, there is no data on the adsorption properties of dibasic calcium silicate hydrate— $\alpha\text{-C}_2\text{SH}$ , which can be easily synthesized from lime and quartz/amorphous silica/silica acid mixtures or from dibasic calcium silicate ( $\text{C}_2\text{S}$ ) polymorphs [22,23]. T. Dambrauskas, K. Baltakys, et al. [24–26] found that  $\alpha\text{-C}_2\text{SH}$  was formed quite easily under hydrothermal conditions in unstirred  $\text{CaO-SiO}_2 \cdot n\text{H}_2\text{O-H}_2\text{O}$  suspensions at  $175\text{--}200\text{ }^\circ\text{C}$  temperature. In fact, while synthesizing  $\alpha\text{-C}_2\text{SH}$ , the intermediary compounds—semi-crystalline C-S-H-type phases are always formed.

Moreover, at a higher temperature and a prolonged reaction time, this compound has been found to recrystallize to kilchoanite ( $\text{Ca}_6(\text{SiO}_4)(\text{Si}_3\text{O}_{10})$ ) and  $\text{C}_8\text{S}_5$  ( $\text{Ca}_8(\text{SiO}_4)_2(\text{Si}_3\text{O}_{10})$ ).

Many studies have been made regarding the properties of  $\alpha\text{-C}_2\text{SH}$ . because of its basis a new hydraulic cementitious materials family has been created (“Celitement”, “solidia Cement”) [27–29]. The main feature of these materials is that the  $\text{CO}_2$  emission and energy consumption associated with cement production can be reduced by up to 30–70%. The production of new cementitious materials is based on a multi-stage process: (1) the synthesis of higher basicity calcium silicate hydrate; (2) activation of the synthesis products and stabilization of highly reactive  $\text{C}_2\text{S}$  forms (“Cellitement”); (3) the cement curing in a water or  $\text{CO}_2$  atmosphere. Moreover, Siauciunas et al. [30] found that an additive of gyrolite intercalated with  $\text{Cd}^{2+}$  ions can be successfully utilized in alternative cement based on  $\alpha\text{-C}_2\text{SH}$ . For these reasons, it is possible to use  $\alpha\text{-C}_2\text{SH}$  with incorporated heavy metal ions in the synthesis of alternative cementitious materials. However, in order to successfully use such material, the first step is to determine and understand their adsorption capacity and its properties.

The aim of this study is to explore the adsorption kinetic parameters of  $\alpha\text{-C}_2\text{SH}$  for  $\text{Co}^{2+}$  ions and its properties.

## 2. Materials and Methods

Fine ground  $\text{SiO}_2 \cdot n\text{H}_2\text{O}$  and calcium oxide were used as starting materials.  $\alpha\text{-C}_2\text{SH}$  was synthesized at  $175\text{ }^\circ\text{C}$  when the duration of isothermal curing was 24 h. The molar ratio of primary mixture ( $\text{CaO}/\text{SiO}_2$ ) was equal to 1.5, while the water/solid ratio was 10. The detailed methodology, the preparation of raw materials, and the formation sequence of intermediate compounds were previously described in works [24–26].

It was determined that the dibasic calcium silicate— $\alpha\text{-C}_2\text{SH}$  (PDF 04-009-6343) and semicrystalline C-S-H type compounds (PDF 00-033-0306 and PDF 00-034-0002) were formed in the synthesis products (Figure 1a). In addition, a small intensity diffraction peaks of calcium carbonate were also identified. X-ray diffraction analysis (XRD) data were proved by the results of simultaneous thermal analysis (STA) (Figure 1b). In the DSC curve, the first endothermic effect ( $50\text{--}200\text{ }^\circ\text{C}$ ) can be assigned to the loss of crystallization water in calcium silicate hydrates. Meanwhile, the decomposition of  $\alpha\text{-C}_2\text{SH}$  is observed in a  $400\text{--}500\text{ }^\circ\text{C}$  temperature interval, in which  $\sim 5.26\%$  of mass were lost (Figure 1b, Curve 1). According to this data, it was calculated that  $\sim 55.5\%$  of  $\alpha\text{-C}_2\text{SH}$  was formed. In addition, two exothermic effects at  $\sim 852$  and  $\sim 872\text{ }^\circ\text{C}$ , which are characteristic of the recrystallization of C-S-H(I) and C-S-H(II) to wollastonite, were identified (Figure 1b, Curve 2). Meanwhile, an endothermic effect at  $\sim 679\text{ }^\circ\text{C}$  was assigned to the decomposition of calcium carbonate. It should be noted that, in further stages of this work, the synthesis product, in which  $\alpha\text{-C}_2\text{SH}$  is the dominant compound, is simply referred to as  $\alpha\text{-C}_2\text{SH}$ .

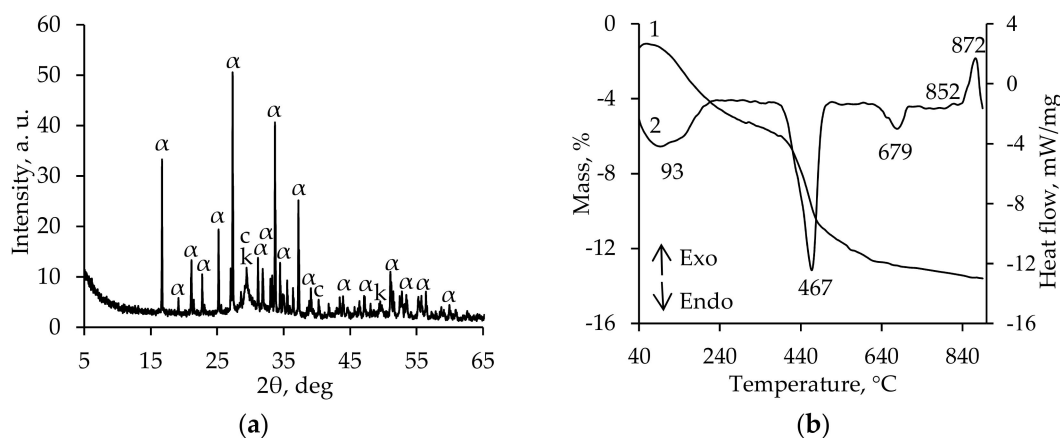


**Figure 1.** XRD pattern (a) and STA curves (Curve 1—TG; Curve 2—DSC) (b) of synthesis product. Indices:  $\alpha$ — $\alpha\text{-C}_2\text{SH}$ ; c— $\text{CaCO}_3$ ; k—C-S-H(I)/C-S-H(II).

The mineralogical composition of samples was determined by X-ray diffraction analysis, while thermal stability was determined by simultaneous thermal analysis, methods that were previously described in works [24–26].

Adsorption experiments were carried out at 25 °C in the thermostatic adsorber Grant Sub14 by stirring 5 g of synthetic  $\alpha$ -C<sub>2</sub>SH in 500 mL of Co(NO<sub>3</sub>)<sub>2</sub>·6H<sub>2</sub>O solutions containing 0.25, 1, or 10 g Co<sup>2+</sup>/dm<sup>3</sup>, when the duration of adsorption varied in a 0.25–30 min range. The pH values of initial Co(NO<sub>3</sub>)<sub>2</sub>·6H<sub>2</sub>O solutions were equal to 6.07 (0.25 g Co<sup>2+</sup>/dm<sup>3</sup>), 4.91 (1 g Co<sup>2+</sup>/dm<sup>3</sup>), and 2.99 (10 g Co<sup>2+</sup>/dm<sup>3</sup>). The concentrations of heavy metal ions were determined using a Perkin-Elmer Analyst 4000 spectrometer (Perkin Elmer, Waltham, MA, USA). The value of pH was measured with a Hanna instrument (Hi 9321, microprocessor pH meter, Hanna Instruments, Woonsocket, RI, USA).

According to S. Zadaviciute et al.'s [16,31] work, the adsorption mechanism of Co<sup>2+</sup> ions by synthetic adsorbents can be determined by pseudo-first-order and pseudo-second-order equations. The pseudo-first-order can be represented by the following equation [31]:

$$\frac{dq_t}{dt} = k_1(q_e - q_t) \quad (1)$$

where  $q_e$  and  $q_t$  are amounts of adsorbed ions at equilibrium and at time  $t_e$ , respectively (mg/g),  $k_1$  is the rate constant of pseudo-first-order adsorption (min<sup>-1</sup>). After integration and applying boundary conditions  $0 \leq t \leq t_e$  and  $0 \leq q_t \leq q_e$ , the integrated form becomes

$$\log(q_e - q_t) = \log q_e - \frac{k_1}{2.303}t. \quad (2)$$

The pseudo-second-order adsorption kinetic rate equation can be expressed as [31]

$$\frac{dq_t}{dt} = k_2(q_e - q_t)^2 \quad (3)$$

where  $k_2$  is the rate constant of the pseudo-second-order adsorption (g/(mg·min)). For the boundary conditions  $0 \leq t \leq t_e$  and  $0 \leq q_t \leq q_e$ , the integrated form of the equation (the integrated rate law for the pseudo-second-order reaction) becomes

$$\frac{t}{q_t} = \frac{1}{kq_e^2} + \frac{1}{q_e}t. \quad (4)$$

### 3. Results and Discussion

In the first part of this work, the adsorption experiment was carried out in a Co(NO<sub>3</sub>)<sub>2</sub>·6H<sub>2</sub>O solution containing 0.25 g Co<sup>2+</sup>/dm<sup>3</sup>. It was determined that the latter process proceeds intensively at the beginning because, after 15 s of reaction, about 50% of cobalt ions were incorporated into the structure of  $\alpha$ -C<sub>2</sub>SH (Figure 2). Moreover, the adsorbed amount of these ions increased and, after 5 min, was equal to 24.68 mg Co<sup>2+</sup>/g  $\alpha$ -C<sub>2</sub>SH. However, the further increment in experiment duration did not affect the uptake of Co<sup>2+</sup> ions because, after 30 min of reaction, the amount of adsorbed ions remained almost the same and was equal to 24.73 mg Co<sup>2+</sup>/g  $\alpha$ -C<sub>2</sub>SH (Figure 2). For this reason, it can be stated that, after 5 min of adsorption, the equilibrium was attained and the adsorption of Co<sup>2+</sup> ions was complete (Figure 2).

It is worth noting that, at the beginning of experiment, about 7.2% (30 mg) of Ca<sup>2+</sup> ions were released from the structure of adsorbent, showing that this dibasic calcium silicate hydrate  $\alpha$ -C<sub>2</sub>SH is unstable in the acidic Co(NO<sub>3</sub>)<sub>2</sub>·6H<sub>2</sub>O solution (Figure 3a). These data can be explained by evaluating the crystal structure of the latter compound. It is well-known that  $\alpha$ -C<sub>2</sub>SH with isolated silicate tetrahedrons possess the lowest degree of polymerization, and its crystal structure consists of isolated acidic SiO<sub>3</sub>(OH) tetrahedra, which share edges with alkaline Ca(O,OH)<sub>6</sub> and Ca(O,OH)<sub>7</sub> polyhedra [32,33]. For this reason, both Ca<sup>2+</sup> cations and OH<sup>-</sup> anions are released, when the structure

of this compound is destroyed in an acidic environment. These data are in a good agreement with the value of pH of liquid medium, which increased from 4.91 (before adsorption) to 6.07 (after 30 min of adsorption). As expected, due to the good adsorption properties of calcium silicate hydrates for metals ions, the concentration of  $\text{Ca}^{2+}$  ions in the liquid medium decreased to 4.56% (18.6 mg) by prolonging the adsorption to 15–30 min.

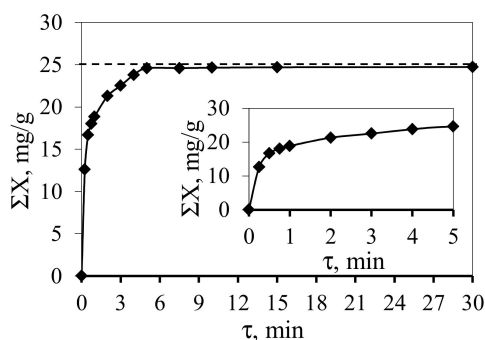


**Figure 2.** Integral kinetic Curve of  $\text{Co}^{2+}$  ion adsorption by  $\alpha\text{-C}_2\text{SH}$ , when the initial concentration of  $\text{Co}^{2+}$  was equal to  $0.25 \text{ g/dm}^3$ .

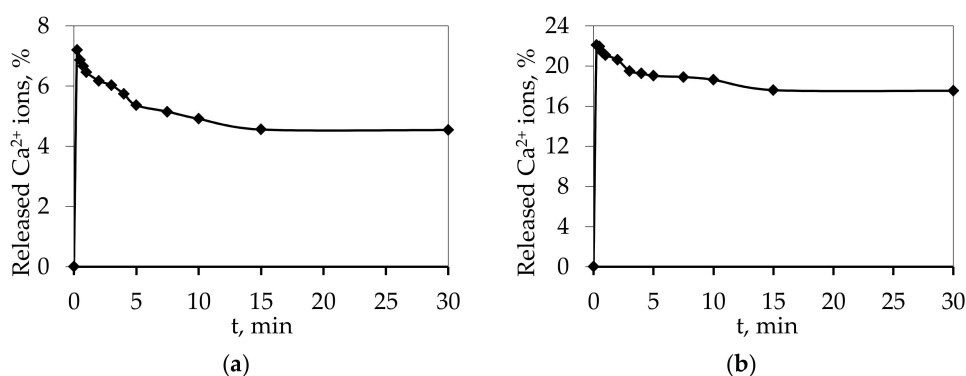


**Figure 3.** The amount of released calcium ions from adsorbent, when the initial concentration of  $\text{Co}^{2+}$  was equal to  $0.25 \text{ g/dm}^3$  (a) and  $1 \text{ g/dm}^3$  (b).

Thus, it is clearly seen that all  $\text{Co}^{2+}$  ions present in liquid medium were adsorbed by  $\alpha\text{-C}_2\text{SH}$  when a lower concentration of  $\text{Co}(\text{NO}_3)_2 \cdot 6\text{H}_2\text{O}$  solution ( $0.25 \text{ g/cm}^3$ ) was used. For this reason, in the next stage of this work, it was raised to  $1 \text{ g of Co}^{2+}/\text{dm}^3$ .

It was determined that a higher metal ion concentration had a positive effect on the incorporation of  $\text{Co}^{2+}$  ions (Figure 4). After 30 s of adsorption,  $\alpha\text{-C}_2\text{SH}$  adsorbed 90% of initial  $\text{Co}^{2+}$  ions ( $90.01 \text{ mg Co}^{2+}/1 \text{ g } \alpha\text{-C}_2\text{SH}$ ) (Figure 4) and released 22.1% (89.84 mg) of  $\text{Ca}^{2+}$  ions (Figure 3b). When the duration of the experiment was extended to 10 min, the equilibrium was attained and the amount of adsorbed ions reached  $99.61 \text{ mg Co}^{2+}/1 \text{ g } \alpha\text{-C}_2\text{SH}$  (Figure 4). Additionally, as in the previous case, the decrease in concentration of desorbed  $\text{Ca}^{2+}$  ions was observed (Figure 3b). It is worth mentioning that, due to a higher destruction of adsorbents, the pH value of liquid medium increased from 4.91 to 10.97. In order to confirm the intercalation of  $\text{Co}^{2+}$  ions, XRF analysis of the adsorbent was performed after 30 min. It was found that the  $\alpha\text{-C}_2\text{SH}$  contained 14.6% of  $\text{Co}^{2+}$  ions.

Thus, the previous results indicated that the interaction between adsorbent and adsorptive followed the addition reaction  $\alpha\text{-C}_2\text{SH} + \text{Co}^{2+} \rightarrow \alpha\text{-C}_2\text{SH} - \text{Co}$ .

In order to determine the maximum adsorption capacity of  $\alpha\text{-C}_2\text{SH}$  for  $\text{Co}^{2+}$  ions, the concentration of  $\text{Co}(\text{NO}_3)_2 \cdot 6\text{H}_2\text{O}$  solution was increased to  $10 \text{ g/dm}^3$ .

It was found that the latter parameter ( $\Sigma x$ ) was equal to  $288 \text{ mg Co}^{2+}/\text{g}$  after 30 min of adsorption, but  $\sim 50\%$  of  $\text{Ca}^{2+}$  ions were released to a liquid medium within the same duration. Thus, due to these

results, it is not recommended that more than 3 g Co<sup>2+</sup>/dm<sup>3</sup> of Co(NO<sub>3</sub>)<sub>2</sub>·6H<sub>2</sub>O solution is used for the adsorption experiments with α-C<sub>2</sub>SH.

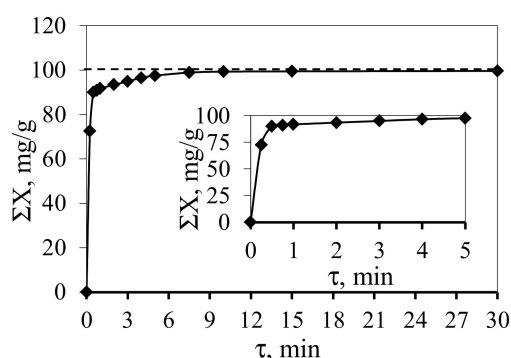


**Figure 4.** Integral kinetic Curve of Co<sup>2+</sup> ion adsorption by α-C<sub>2</sub>SH when the initial concentration of Co<sup>2+</sup> was equal to 1 g/dm<sup>3</sup>.

According to the literature, the adsorption capacity of lower basicity calcium silicate hydrates (gyrolite, xonotlite, and tobermorite) depends on the nature of adsorptive. Kasperavičiute et al. [34] determined that the maximum amount of adsorbed Cu<sup>2+</sup> ions by gyrolite is equal to 1480 mg Cu<sup>2+</sup>/g. Meanwhile, Bankauskaite et al. [35] showed that the adsorption capacity of this compound for Co<sup>2+</sup> ions is equal only to 14 mg Co<sup>2+</sup>/g. For this reason, it can be stated that synthetic α-C<sub>2</sub>SH can be used as an adsorbent for cobalt ions.

In order to determine if adsorption is a reversible process or not in a neutral liquid medium, α-C<sub>2</sub>SH sample with intercalated Co<sup>2+</sup> ions (1 g Co<sup>2+</sup>/dm<sup>3</sup>) was dried up and immersed in distilled water. It was measured that, after 60 min at 25 °C, Co<sup>2+</sup> ion concentrations in the solution did not exceed ~0.008%. It is worth mentioning that, after the desorption process, 14.6 wt % Co<sup>2+</sup> ions were detected in the α-C<sub>2</sub>SH structure via XRF analysis.

Furthermore, in the next stage of this research, the kinetic adsorption parameters were determined by applying pseudo-first-order and pseudo-second-order equations. Solutions containing 0.25 g and 1 g Co<sup>2+</sup>/dm<sup>3</sup> were chosen. The aforementioned equation suitability for the adsorption reaction was verified by comparing the calculated equilibrium concentrations ( $q_{e(cal)}$ ) of Co<sup>2+</sup> ions to the experimental concentrations ( $q_{e(exp)}$ ). In addition, the equation is suitable only if the errors between  $q_{e(cal)}$  and  $q_{e(exp)}$  do not exceed 5%.

Using the pseudo-first-order equation, it was found that the values of  $R^2$  were lower (0.84, 0.86) and that the values of  $q_{e(cal)}$  disagreed with the experimental  $q_{e(exp)}$  ones (Table 1). Thus, the pseudo-first-order equation did not fit well with the Co<sup>2+</sup> ion adsorption mechanism description.

**Table 1.** The kinetic parameters of the pseudo-first- and pseudo-second-order kinetic models.

Concentration (g Co <sup>2+</sup> /dm <sup>3</sup> )	$R^2$	$q_{e(exp)}$ (mg/g)	$q_{e(cal)}$ (mg/g)	$k_1$ (min <sup>-1</sup> )	$k_2$ (g/(mg·min))
<b>Pseudo-First-Order Kinetic Models</b>					
0.25	0.84	24.73	8.39	0.450	-
1.00	0.85	99.62	16.93	0.356	-
<b>Pseudo-Second-Order Kinetic Models</b>					
0.25	1.00	24.73	25.08	-	0.139
1.00	1.00	99.62	100.00	-	0.091

Different results were obtained using the pseudo-second-order kinetics equation: the values of  $R^2$  were near 1 and equal to 0.99 (0.25 g Co<sup>2+</sup>/dm<sup>3</sup>) and 1.00 (1 g Co<sup>2+</sup>/dm<sup>3</sup>) (Figure 5). In addition, the calculated  $q_{e(cal)}$  values were close to the experimental  $q_{e(exp)}$  ones (Table 1). Thus, it can be stated

that pseudo-second-order kinetics model adequately describes the  $\text{Co}^{2+}$  ion adsorption mechanism of  $\alpha\text{-C}_2\text{SH}$ . Moreover, it was calculated that the  $\text{Co}^{2+}$  ion adsorption rate ( $k_2 = 0.139 \text{ g}/(\text{mg}\cdot\text{min})$ ) is higher in the solution containing  $0.25 \text{ g Co}^{2+}/\text{dm}^3$  than in the solution containing  $1 \text{ g Co}^{2+}/\text{dm}^3$  ( $k_2 = 0.091 \text{ g}/(\text{mg}\cdot\text{min})$ ) (Table 1). It should be noted that these data agree with the experimental results and confirm that  $\text{Co}^{2+}$  ions are chemisorbed by  $\alpha\text{-C}_2\text{SH}$ . The same phenomenon can be found in the literature [31,34–38].

In order to evaluate the stability of the adsorbent,  $\alpha\text{-C}_2\text{SH}$  was described by X-ray diffraction and simultaneous thermal analysis. It was determined that, after the adsorption process, in the solution containing  $0.25$  and  $1 \text{ g Co}^{2+}/\text{dm}^3$ , the intensity of the main diffraction peaks characteristic to  $\alpha\text{-C}_2\text{SH}$  decreased by 1.77 and 2.53 times, respectively (Figures 1a and 6). In addition,  $89.84 \text{ mg}$  of  $\text{Ca}^{2+}$  ions were desorbed from the crystal structure of  $\alpha\text{-C}_2\text{SH}$ . However, the structure of the latter compound remained stable. Meanwhile, after adsorption in the solution containing  $10 \text{ g Co}^{2+}/\text{dm}^3$ ,  $\alpha\text{-C}_2\text{SH}$  fully decomposed because diffraction peaks typical to this compound are not detected in XRD patterns (Figure 6). It is worth mentioning that two diffraction peaks characteristic to a new compound were observed, but it was impossible to identify it.

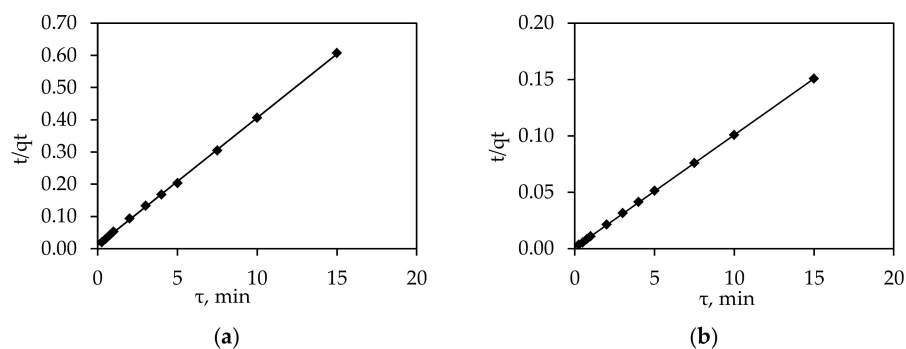


**Figure 5.** Pseudo-second-order kinetic plots, when the initial concentration of  $\text{Co}^{2+}$  was equal to  $0.25 \text{ g}/\text{dm}^3$  (a) and  $1 \text{ g}/\text{dm}^3$  (b).

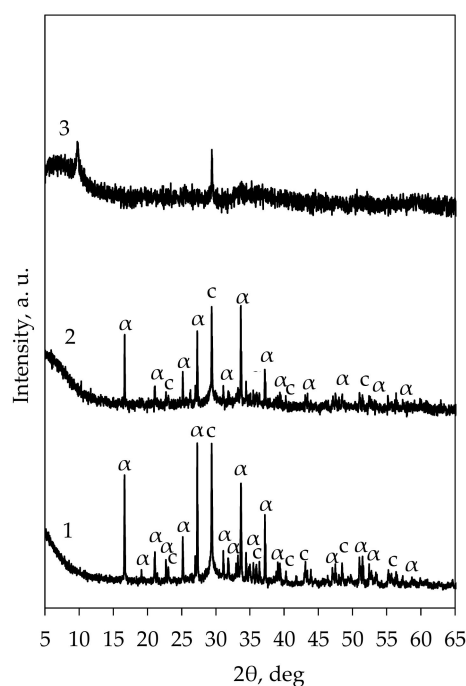


**Figure 6.** XRD curves of  $\alpha\text{-C}_2\text{SH}$  after the adsorption process, when the initial concentration of  $\text{Co}^{2+}$  was equal to  $0.25 \text{ g}/\text{dm}^3$  (Curve 1),  $1 \text{ g}/\text{dm}^3$  (Curve 2), and  $10 \text{ g}/\text{dm}^3$  (Curve 3).

XRD results were supported by STA analysis data. It was found that the absorbed heat of the first endothermic effect increased from 84.26 (pure  $\alpha$ -C<sub>2</sub>SH) (Figure 1b) to 175.78 J/g ( $\alpha$ -C<sub>2</sub>SH after adsorption in solution containing 10 g Co<sup>2+</sup>/dm<sup>3</sup>) (Figure 7). These data can be associated with the amorphization of the synthesis product. Meanwhile, the quantity of  $\alpha$ -C<sub>2</sub>SH decreased by 1.8 times after adsorption in solutions with lower Co<sup>2+</sup> ion concentrations. Meanwhile, the endothermic effect typical to this compound was not identified in DSC curves of sample, in which the 10 g/dm<sup>3</sup> Co(NO<sub>3</sub>)<sub>2</sub>·6H<sub>2</sub>O solution was used (Figure 7c). This clearly shows that  $\alpha$ -C<sub>2</sub>SH is fully decomposed in such an acidic environment. It was found that semicrystalline calcium silicate hydrates—C-S-H(I) and C-S-H(II)—decomposed after adsorption in solution containing 1 g Co<sup>2+</sup>/dm<sup>3</sup> (Figure 7). It is worth mentioning that, during the adsorption process, carbonization appeared, and the quantity of calcium carbonate increased to 6.75–9% (Figure 7).

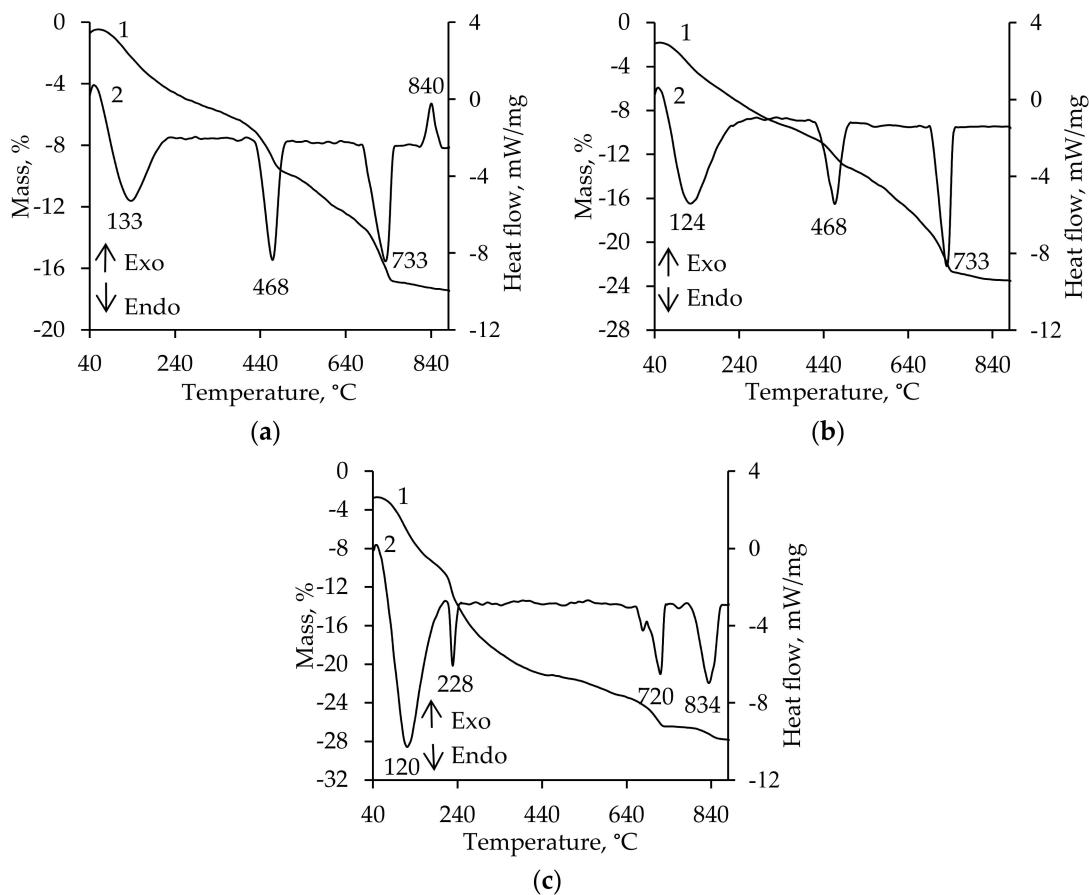


**Figure 7.** STA curves (Curve 1—TG; Curve 2—DSC) of  $\alpha$ -C<sub>2</sub>SH after adsorption process, when the initial concentration of Co<sup>2+</sup> was equal to 0.25 g/dm<sup>3</sup> (a); 1 g/dm<sup>3</sup> (b); and 10 g/dm<sup>3</sup> (c).

In further research,  $\alpha$ -C<sub>2</sub>SH with incorporated Co<sup>2+</sup> ions will be used in alternative cementitious materials, and the properties of these binder materials such as hydration, mineralogical composition, and porosity will be examined.

#### 4. Conclusions

It was obtained, that the adsorption capacity of  $\alpha$ -C<sub>2</sub>SH and intrusion of Co<sup>2+</sup> ions in its structure depends on the reaction time and the initial concentration of metal ions. It was determined that the highest value of adsorbed metal ions by 1 g of  $\alpha$ -C<sub>2</sub>SH was equal to 288 mg. It was found that interaction between adsorbent and adsorptive follows the addition reaction:  $\alpha$ -C<sub>2</sub>SH + Co<sup>2+</sup> →  $\alpha$ -C<sub>2</sub>SH - Co.

It was observed that the pseudo-second-order model fit well with the cobalt ion adsorption mechanism description, because the calculated  $q_{e(\text{cal})}$  values were close to the experimental  $q_{e(\text{exp})}$  ones. By the way, it was found that the  $\text{Co}^{2+}$  ion adsorption rate ( $k_2$ ) depends on the initial metal ion concentration. It was determined that the adsorption reactions are not reversible in a neutral liquid medium, because after desorption experiment,  $\text{Co}^{2+}$  ion concentrations in the solution did not exceed ~0.008%.

**Acknowledgments:** This research was funded by a Grant (No. S-MIP-17-92) from the Research Council of Lithuania.

**Author Contributions:** The paper was written through contributions of all authors. T.D. synthesized  $\alpha\text{-C}_2\text{SH}$ , while D.N. performed the adsorption experiment. T.D. and K.B. performed TGA and XRD experiments. The project oversight, data analysis, result interpretation, and manuscript writing were performed by all authors.

**Conflicts of Interest:** The authors declare no conflict of interest.

## References

1. Wang, J.; Chen, C. Biosorbents for heavy metals removal and their future. *Biotechnol. Adv.* **2009**, *27*, 195–226. [[CrossRef](#)] [[PubMed](#)]
2. Aguado, J.; Arsuaga, J.A.; Arencibia, A.; Lindo, M.; Gascón, V. Aqueous heavy metals removal by adsorption on amine-functionalized mesoporous silica. *J. Hazard. Mater.* **2009**, *163*, 213–221. [[CrossRef](#)] [[PubMed](#)]
3. Repo, E.; Warchoń, J.K.; Bhatnagar, A.; Sillanpää, M. Heavy metals adsorption by novel EDTA-modified chitosan–silica hybrid materials. *J. Colloid Interface Sci.* **2011**, *358*, 261–267. [[CrossRef](#)] [[PubMed](#)]
4. Barakat, M.A. New trends in removing heavy metals from industrial wastewater. *Arab. J. Chem.* **2011**, *4*, 361–377. [[CrossRef](#)]
5. Kadirvelu, K.; Thamaraiselvi, K.; Namasivayam, C. Removal of heavy metals from industrial wastewaters by adsorption onto activated carbon prepared from an agricultural solid waste. *Bioresour. Technol.* **2001**, *75*, 63–65. [[CrossRef](#)]
6. Fenglian, F.; Wang, Q. Removal of heavy metal ions from wastewaters: A review. *J. Environ. Manag.* **2011**, *92*, 407–418. [[CrossRef](#)]
7. Sud, D.; Mahajan, G.; Kaur, M.P. Agricultural waste material as potential adsorbent for sequestering heavy metal ions from aqueous solutions—A review. *Bioresour. Technol.* **2008**, *99*, 6017–6027. [[CrossRef](#)] [[PubMed](#)]
8. Wan Ngah, W.S.; Hanafiah, M.A.K.M. Removal of heavy metal ions from wastewater by chemically modified plant wastes as adsorbents: A review. *Bioresour. Technol.* **2008**, *99*, 3935–3948. [[CrossRef](#)] [[PubMed](#)]
9. Ajmal, M.; Rao, R.A.K.; Anwar, S.; Ahmad, J.; Ahmad, R. Adsorption studies on rice husk: Removal and recovery of Cd(II) from wastewater. *Bioresour. Technol.* **2003**, *86*, 147–149. [[CrossRef](#)]
10. Argun, M.E.; Dursun, S.; Ozdemir, C.; Karatas, M. Heavy metal adsorption by modified oak sawdust: Thermodynamics and kinetics. *J. Hazard. Mater.* **2007**, *141*, 77–85. [[CrossRef](#)] [[PubMed](#)]
11. Šćiban, M.; Radetić, B.; Kevrešan, Ž.; Klačnja, M. Adsorption of heavy metals from electroplating wastewater by wood sawdust. *Bioresour. Technol.* **2007**, *98*, 402–409. [[CrossRef](#)] [[PubMed](#)]
12. Zhao, J.; Zhu, Y.J.; Wu, J.; Zheng, J.Q.; Zhao, Z.Y.; Lu, B.Q.; Chen, F. Chitosan-coated mesoporous microspheres of calcium silicate hydrate: Environmentally friendly synthesis and application as a highly efficient adsorbent for heavy metal ions. *J. Colloid Interface Sci.* **2014**, *418*, 208–215. [[CrossRef](#)] [[PubMed](#)]
13. Belmabkhout, Y.; Serna-Guerrero, R.; Sayari, A. Adsorption of  $\text{CO}_2$ -Containing Gas Mixtures over Amine-Bearing Pore-Expanded MCM-41 Silica: Application for Gas Purification. *Ind. Eng. Chem. Res.* **2010**, *49*, 359–365. [[CrossRef](#)]
14. Guo, Y.; Qi, J.; Yang, S.; Yu, K.; Wang, Z.; Xu, H. Adsorption of Cr(VI) on micro- and mesoporous rice husk-based active carbon. *Mater. Chem. Phys.* **2003**, *78*, 132–137. [[CrossRef](#)]
15. Cavenati, S.; Grande, C.A.; Rodrigues, A.E. Adsorption Equilibrium of Methane, Carbon Dioxide, and Nitrogen on Zeolite 13X at High Pressures. *J. Chem. Eng. Data* **2004**, *49*, 1095–1101. [[CrossRef](#)]
16. Zadaviciute, S.; Bankauskaite, A.; Baltakys, K.; Eisinias, A. The study of CP determination of hydrotalcite intercalated with heavy metal ions. *J. Therm. Anal. Calorim.* **2017**. [[CrossRef](#)]
17. Yong, S.O.; Yang, J.E.; Zhang, Y.S.; Kim, S.J.; Chung, D.Y. Heavy metal adsorption by a formulated zeolite-Portland cement mixture. *J. Hazard. Mater.* **2007**, *147*, 91–96. [[CrossRef](#)]

18. Wu, J.; Zhu, Y.J.; Cao, S.W.; Chen, F. Hierarchically nanostructured mesoporous spheres of calcium silicate hydrate: Surfactant-free sonochemical synthesis and drug-delivery system with ultrahigh drug-loading capacity. *Adv. Mater.* **2010**, *22*, 749–753. [CrossRef] [PubMed]
19. Wu, J.; Zhu, Y.J.; Chen, F. 45S5 Bioglass-derived glass-ceramic scaffolds for bone tissue engineering. *Biomaterials* **2006**, *27*, 2414–2425. [CrossRef]
20. Eisinas, A.; Baltakys, K.; Siauciunas, R. Utilisation of gyrolite with impure  $\text{Cd}^{2+}$  ions in cement stone. *Adv. Cem. Res.* **2013**, *25*, 69–79. [CrossRef]
21. Eisinas, A.; Baltakys, K.; Siauciunas, R. Removal of Zn(II), Cu(II) and Cd(II) from aqueous solution using gyrolite. *J. Sci. Ind. Res.* **2012**, *71*, 566–572.
22. Ishida, H.; Yamazaki, S.; Sasaki, K.; Okada, Y.; Mitsuda, T.  $\alpha$ -Dicalcium Silicate Hydrate—Preparation, Decomposed Phase and Its Hydration. *J. Am. Ceram. Soc.* **1993**, *76*, 1707–1712. [CrossRef]
23. Garbev, K.; Gasharova, B.; Beuchle, G.; Kreiszi, S.; Stemmermann, P. First Observation of  $\alpha\text{-Ca}_2[\text{SiO}_3(\text{OH})](\text{OH})\text{-Ca}_6[\text{Si}_2\text{O}_7][\text{SiO}_4](\text{OH})_2$  Phase Transformation upon Thermal Treatment in Air. *J. Am. Ceram. Soc.* **2008**, *91*, 263–271. [CrossRef]
24. Baltakys, K.; Dambrauskas, T.; Eisinas, A. The Synthesis of  $\alpha\text{-C}_2\text{S}$  Hydrate Substituted with  $\text{Al}^{3+}$  Ions in Mixture with  $\text{CaO/SiO}_2 = 1.75$ . *Solid State Phenom.* **2015**, *244*, 26–33. [CrossRef]
25. Dambrauskas, T.; Baltakys, K.; Eisinas, A.; Siauciunas, R. A study on the thermal stability of kilchoanite synthesized under hydrothermal conditions. *J. Therm. Anal. Calorim.* **2017**, *127*, 229–238. [CrossRef]
26. Dambrauskas, T.; Baltakys, K.; Eisinas, A. Formation and thermal stability of calcium silicate hydrate substituted with  $\text{Al}^{3+}$  ions in the mixtures with  $\text{CaO/SiO}_2 = 1.5$ . *J. Therm. Anal. Calorim.* **2017**. [CrossRef]
27. Sahu, S.; DeCristofaro, N. Part one of a two-part series exploring the chemical properties and performance results of Sustainable Solidia Cement™ and Solidia Concrete™. *Solidia Cem.* **2013**, 1–12. Available online: <http://solidiatech.com/wp-content/uploads/2014/02/Solidia-Cement-White-Paper-12-17-13-FINAL.pdf> (accessed on 15 January 2018).
28. Barcelo, L.; Kline, J.; Walenta, G.; Gartner, E. Cement and carbon emissions. *Mater. Struct.* **2014**, *47*, 1055–1065. [CrossRef]
29. Gartner, E.; Hirao, H. A review of alternative approaches to the reduction of  $\text{CO}_2$  emissions associated with the manufacture of the binder phase in concrete. *Cem. Concr. Res.* **2015**, *78*, 126–142. [CrossRef]
30. Siauciunas, R.; Baltakys, K.; Gendvilas, R.; Eisinas, A. The influence of Cd-impure gyrolite on the hydration of composite binder material based on  $\alpha\text{-C}_2\text{S}$  hydrate. *J. Therm. Anal. Calorim.* **2014**, *118*, 857–863. [CrossRef]
31. Zadaviciute, S.; Baltakys, K.; Eisinas, A.; Bankauskaite, A. Simultaneous adsorption at 25 °C and the peculiarities of gyrolite substituted with heavy metals. *J. Therm. Anal. Calorim.* **2017**, *127*, 335–343. [CrossRef]
32. Garbev, K.; Black, L.; Beuchle, G.; Stemmermann, P. Inorganic Polymers in Cement Based Materials. *Wasser Geotechnol.* **2002**, *1*, 19–30.
33. Garbev, K.; Gasharova, B.; Stemmermann, P. A Modular Concept of Crystal Structure Applied to the Thermal Transformation of  $\alpha\text{-C}_2\text{SH}$ . *J. Am. Ceram. Soc.* **2014**, *97*, 2286–2297. [CrossRef]
34. Kasperaviciute, V.; Baltakys, K.; Siauciunas, R. the sorption properties of gyrolite for copper ions. *Ceram. Silikáty* **2008**, *52*, 95–101.
35. Bankauskaite, A.; Eisinas, A.; Baltakys, K.; Zadaviciute, S. A study on the intercalation of heavy metal ions in a wastewater by synthetic layered inorganic adsorbents. *Desalin. Water Treat.* **2015**, *56*, 1576–1586. [CrossRef]
36. Pradhan, N.; Rene, E.R.; Lens, P.N.L.; Dipasquale, L.; D'Ippolito, G.; Fontana, A.; Panico, A.; Esposito, G. Adsorption Behaviour of Lactic Acid on Granular Activated Carbon and Anionic Resins: Thermodynamics, Isotherms and Kinetic Studies. *Energies* **2017**, *10*, 665. [CrossRef]
37. Ho, Y.S.; Wase, D.A.J.; Forster, C.F. Batch Nickel Removal from Aqueous Solution by Sphagnum Moss Peat. *Water Res.* **1995**, *29*, 1327–1332. [CrossRef]
38. Ho, Y.S.; Wase, D.A.J.; Forster, C.F. Kinetic Studies of Competitive Heavy Metal Adsorption by Sphagnum Moss Peat. *Environ. Technol.* **1996**, *17*, 71–77. [CrossRef]

